OUKA
The University of Osaka
Institutional Knowledge Archive

Title	A Ku band pulsed electron paramagnetic resonance spectrometer using an arbitrary waveform generator for quantum control experiments at millikelvin temperatures
Author(s)	Yap, Yung Szen; Tabuchi, Yutaka; Negoro, Makoto et al.
Citation	Review of Scientific Instruments. 2015, 86(6), p. 063110
Version Type	VoR
URL	https://hdl.handle.net/11094/77647
rights	
Note	

The University of Osaka Institutional Knowledge Archive : OUKA

https://ir.library.osaka-u.ac.jp/

The University of Osaka

Review of Scientific Instruments

A Ku band pulsed electron paramagnetic resonance spectrometer using an arbitrary waveform generator for quantum control experiments at millikelvin temperatures

Cite as: Rev. Sci. Instrum. **86**, 063110 (2015); https://doi.org/10.1063/1.4922791
Submitted: 28 April 2015 . Accepted: 07 June 2015 . Published Online: 24 June 2015

Yung Szen Yap, Yutaka Tabuchi, Makoto Negoro, Akinori Kagawa, and Masahiro Kitagawa

View Online Export Citation CrossMark

ARTICLES YOU MAY BE INTERESTED IN

Inductive-detection electron-spin resonance spectroscopy with 65 spins/ $\sqrt{\text{Hz}}$ sensitivity
Applied Physics Letters **111**, 202604 (2017); https://doi.org/10.1063/1.5002540

An X-band pulsed electron paramagnetic resonance spectrometer with time resolution improved by a field-programmable-gate-array based pulse generator
Review of Scientific Instruments **89**, 125104 (2018); https://doi.org/10.1063/1.5048551

Superconducting coplanar waveguide resonators for low temperature pulsed electron spin resonance spectroscopy
Review of Scientific Instruments **84**, 025116 (2013); https://doi.org/10.1063/1.4792205

© 2015 AIP Publishing LLC.

A Ku band pulsed electron paramagnetic resonance spectrometer using an arbitrary waveform generator for quantum control experiments at millikelvin temperatures

Yung Szen Yap,[1,2,a)] Yutaka Tabuchi,[3] Makoto Negoro,[1] Akinori Kagawa,[1] and Masahiro Kitagawa[1,b)]
[1]*Graduate School of Engineering Science, Osaka University, 1-3 Machikaneyama-cho, Toyonaka-shi, Osaka 560-8531, Japan*
[2]*Faculty of Science, Universiti Teknologi Malaysia, 81310 UTM Johor Bahru, Johor, Malaysia*
[3]*Research Center for Advanced Science and Technology (RCAST), The University of Tokyo, Meguro-ku, Tokyo 153-8904, Japan*

(Received 28 April 2015; accepted 7 June 2015; published online 24 June 2015)

We present a 17 GHz (Ku band) arbitrary waveform pulsed electron paramagnetic resonance spectrometer for experiments down to millikelvin temperatures. The spectrometer is located at room temperature, while the resonator is placed either in a room temperature magnet or inside a cryogen-free dilution refrigerator; the operating temperature range of the dilution unit is from ca. 10 mK to 8 K. This combination provides the opportunity to perform quantum control experiments on electron spins in the pure-state regime. At 0.6 T, spin echo experiments were carried out using γ-irradiated quartz glass from 1 K to 12.3 mK. With decreasing temperatures, we observed an increase in spin echo signal intensities due to increasing spin polarizations, in accordance with theoretical predictions. Through experimental data fitting, thermal spin polarization at 100 mK was estimated to be at least 99%, which was almost pure state. Next, to demonstrate the ability to create arbitrary waveform pulses, we generate a shaped pulse by superposing three Gaussian pulses of different frequencies. The resulting pulse was able to selectively and coherently excite three different spin packets simultaneously—a useful ability for analyzing multi-spin system and for controlling a multi-qubit quantum computer. By applying this pulse to the inhomogeneously broadened sample, we obtain three well-resolved excitations at 8 K, 1 K, and 14 mK. © *2015 AIP Publishing LLC.* [http://dx.doi.org/10.1063/1.4922791]

I. INTRODUCTION

Most pulsed electron paramagnetic resonance (EPR) spectrometers are capable of generating only simple pulses, i.e., rectangular pulses of fixed amplitude and phase. Such pulses have poor frequency-selectivity and are prone to have systematic errors, often leading to unwanted spin evolution. In nuclear magnetic resonance (NMR), these problems are normally solved using advanced pulses,[1] often with varying amplitudes or phase profiles, e.g., composite pulses,[2–4] shaped pulses,[5–7] and numerically optimized modulated pulses.[8] NMR spectrometers are also used to generate selective, multi-frequency pulses for experiments with multi-spin systems, e.g., Hadamard spectroscopy and quantum computation.[9,10] To create such complex pulses for EPR experiments, spectrometers capable of generating arbitrary waveform pulses have been developed, mostly at X band frequencies for experiments at various temperatures.[11–20]

Low temperatures are particularly useful to reduce thermal noise of microwave components and increase thermal spin polarization, which improve signal-to-noise ratio (SNR). While improved SNR is advantageous, some experiments require high polarizations for specific reasons, e.g., molecular spin quantum computation[21,22] requires polarization above 99%, which is almost pure state, to initialize qubits, while simultaneously requiring the use of advanced pulse techniques to achieve precise spin control.[1,23–28] Thermal equilibrium polarization P, for a spin 1/2 system at temperature T, is given by

$$P = \tanh\left(\frac{\hbar\gamma_e B_0}{2k_B T}\right), \tag{1}$$

where $\hbar$ is the reduced Planck's constant, γ_e is electron gyromagnetic ratio, B_0 is the externally applied magnetic field strength, and k_B is Boltzmann constant. For example, for EPR setups operating at 250 GHz ($B_0 \approx 8.9$ T, assuming electron g-factor, $g = 2.003$), almost unity polarization ($P \geq 99\%$) is attainable at 2 K.[29–32] However, precise spin control at frequencies above 50 GHz (V band and above) is technically challenging. On the contrary, lower frequencies are based on mature technology, which provides for a multitude of readily available components and techniques. Inevitably, temperatures lower than 450 mK are necessary to polarize electron spins beyond 99% for setups below 50 GHz (Q band and below).

The ability to create complex pulses to precisely control initialized spins has motivated us in our present work. In this paper, we present an arbitrary waveform EPR spectrometer, operating at ca. 17 GHz (Ku band) for experiments with the

a)Electronic mail: yungszen@utm.my
b)Electronic mail: kitagawa@ee.es.osaka-u.ac.jp

 © 2015 AIP Publishing LLC

resonator placed either in a room temperature magnet or in a dilution refrigerator for low temperature experiments. Using spin echoes on a γ-irradiated quartz glass sample, we show that signal intensities increase with decreasing temperature in accordance with Eq. (1) and demonstrate almost unity polarization by cooling the sample down to millikelvin temperatures. Next, we demonstrate the ability to create and apply shaped pulses to the cooled sample. To do so, we superpose three Gaussian shaped pulses, each at a different frequency, to obtain three coherent and well-resolved excitations at millikelvin temperatures.

II. INSTRUMENT DESIGN

The home-built setup is presented in Fig. 1. First, frequency and amplitude modulated pulses were numerically designed and digitally generated at 2.5 GHz (1.5 GHz bandwidth) using an arbitrary waveform generator (AWG). Next, it was up-converted by mixing it with a ca. 14 GHz signal generated from a local oscillator. The resulting signal was filtered using a high pass filter, amplified using a broadband traveling-wave tube amplifier (TWTA), and directed into the resonator. The setup has an operating frequency range of 16.5–18.0 GHz, determined by the cutoff frequency of the high pass filter (16.5 GHz) and the upper frequency limit of the TWTA waveguide output (18.0 GHz). The TWTA output was attenuated using a variable attenuator (CVA13-20D) and an isolator was installed after the variable attenuator to prevent any reflected signals from re-entering and damaging the TWTA (refer to Fig. 1).

The setup was configured for transmission measurements with the resonator placed either in a room temperature magnet or in a cryogen-free dilution refrigerator.[34] This configuration, however, can be easily converted to a reflection system by using a circulator and a reflection-type resonator. A 3.5 m long low-loss coaxial cable was used to connect the TWTA output to the SubMiniature version A (SMA) port of the dilution refrigerator; excluding the variable attenuator, the total attenuation was around 2.8 dB.

The room temperature SMA ports in the dilution refrigerator were connected to the Pulse-Tube 2 (PT2) stage (see Fig. 1) using low thermal conductivity coaxial cables, consisting of a silver-plated phosphor bronze core with an outer stainless steel shield (TCR219CG/SUS by Kawashima Manufacturing Co., Ltd.). Superconducting Nb coaxial cables (SC-219/50-Nb-Nb by Coax Co., Ltd.) were installed from the PT2 stage to the mixing chamber (MC) stage. To thermally anchor the cables to their respective stages, 1 dB attenuators were installed at PT1, PT2, still, and MC stages. These attenuators helped to conduct heat away from the inner conductor and prevent a direct thermal connection from room temperature to the MC stage through the superconducting coaxial cables. At 12.5 mK, the total attenuation from the room temperature SMA ports to the MC stage was approximately 6.5 dB. In addition, the dilution refrigerator was fitted with a 5 T superconducting magnet (resolution = 1 G), which was attached to the PT2 stage. At the MC stage of the dilution refrigerator, the lowest attainable temperature was about 10 mK and the cooling power at 100 mK was about 300 μW (with 3 mW of power applied to the heater installed at the still stage).

The resonator was thermally connected to the MC stage (see Fig. 2), where precise and stable temperature control was achieved using a temperature controller (Model 370AC by Lakeshore). Temperatures up to 8 K were obtained by direct heating of the MC stage, while other stages (except PT1 stage) remained well below 4 K; hence, superconductivity of the magnet and cables was not lost.

From the dilution refrigerator's SMA port, another 3.5 m long low-loss cable was used to direct signals back into the receiver. In the receiving end, signals from the spins were amplified using two Ku band low noise amplifiers (LNAs) with

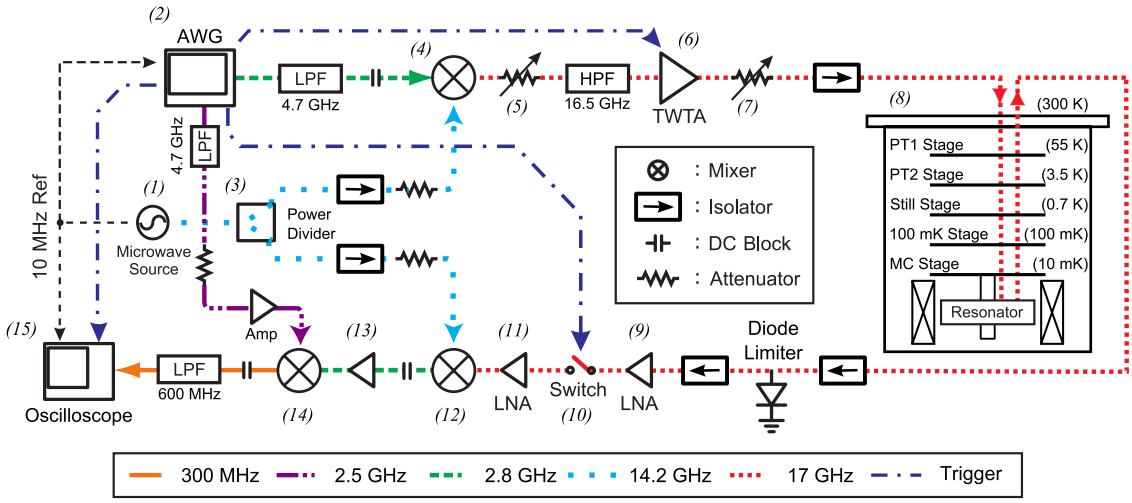

FIG. 1. Schematic of the home-built pulsed EPR spectrometer. The major components labeled with italicized numbers in parentheses are: (1) microwave source (83623B by Agilent Technologies), (2) arbitrary waveform generator (AWG7102 by Tektronix, Inc.), (3) power divider (1515-1 by Aeroflex Weinschel), (4) triple balanced microwave mixer (M3206L by Advanced Microwave, Inc.), (5) variable attenuator (9804-20 by ARRA, Inc.), (6) traveling-wave tube amplifier (TWTA) (176 Ku by Applied Systems Engineering, Inc.),[33] (7) variable attenuator (CVA13-20D by Microwave Communications Laboratories, Inc.), (8) magnet in dilution refrigerator (Triton 400 by Oxford Instruments) or room temperature magnet (9) Ku band low noise amplifier (BZ1218LC1 by B&Z Technologies), (10) high speed PIN switch (PSH-42 by Millitech, Inc.), (11) Ku band low noise amplifier (BZ1218LC1 by B&Z Technologies), (12) double balanced mixer (AM10620-LA by AtlanTecRF), (13) radio-frequency amplifier (AD8353 by Analog Devices, Inc.), (14) frequency mixer (ZX05-30W+ by Mini-Circuits, Inc.), and (15) oscilloscope (DPO7254 by Tektronix, Inc.).

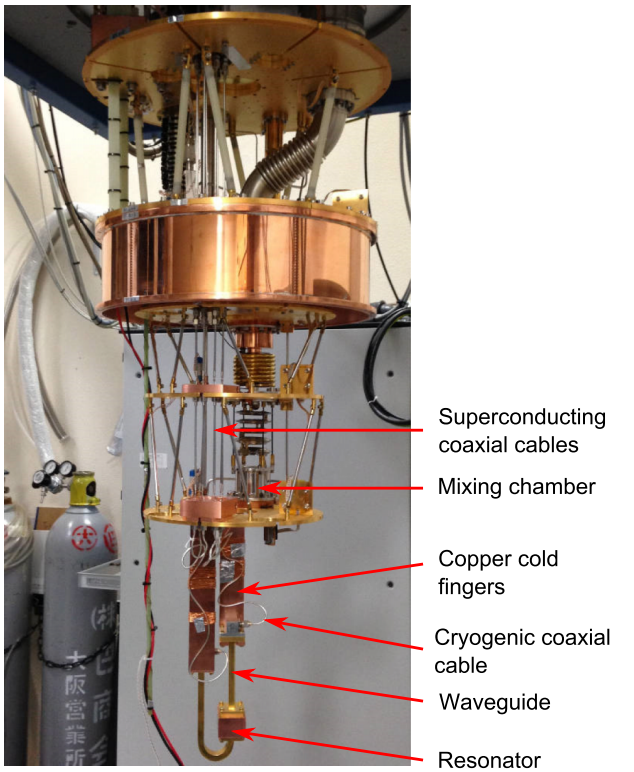

FIG. 2. The mounted resonator in the cryogen-free dilution refrigerator. This photo shows the bare dilution refrigerator without the superconducting magnet, radiation shields, thermal insulators, and vacuum cans. Below the MC stage, copper cold fingers supported and conducted heat away from the coaxial cables, waveguides, and resonators. The coaxial cables were thermally anchored to the cold fingers using uncoated copper wires and cryogenic grease was applied to all contact surfaces of the cold fingers.

a rated noise figure of 1.1 dB and a typical gain of 30 dB at 18 GHz. The signal was then down-converted to 2.8 GHz and amplified again. Finally, the signal was down-converted to 300 MHz before it was sampled using an 8-bit digital oscilloscope at a sampling rate of 10 GS/s. Both AWG and oscilloscope were referenced to the local oscillator's 10 MHz reference signal. To minimize risk of self oscillation within the spectrometer, a high speed PIN microwave switch was installed at the receiver and isolators were placed in between the power divider output ports and the mixers' local oscillator (LO) ports. DC blocks were installed to protect the mixers since some balanced mixers contain a transformer in the intermediate frequency (IF) ports, which is easily damaged by DC voltages. A diode limiter was installed to protect the LNAs from high voltages and any reflected signal was absorbed by another isolator placed before the diode limiter. For noise figure optimization, some LNAs may have slightly different input impedance. To absorb any reflected signals due to the impedance mismatch, an isolator was installed in front of the first LNA.

The AWG was configured to run with two 8-bit digital-to-analog output channels at a sampling rate of 10 GS/s (thus, time resolution = 0.1 ns) and 3 triggers to control the microwave switch, TWTA, and oscilloscope. A home-built software compiler made using C++ language allowed users to create arbitrary waveforms using 3 input parameters: amplitude (dynamic range of 30 dB), phase (resolution = 1°), and pulse

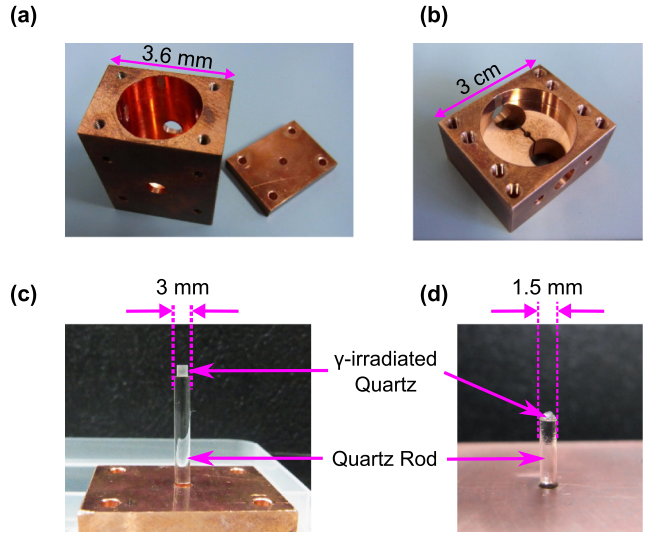

FIG. 3. The cylindrical cavity (a) and loop gap resonator (b) that were used for low temperature experiments, along with the respective samples (c) and (d). Both resonators were tested with γ-irradiated quartz glass, which were attached quartz glass rods using cryogenic grease.

duration (resolution = 1 ns). In our previous work,[35] this setup was used successfully to average 10 000 free induction decay signals at room temperature.

III. RESONATOR AND SAMPLE

The paramagnetic species used in all of the experiments reported here were defect centers found in γ-irradiated quartz glass. This material was chosen because it is widely used as a standard sample for pulsed EPR, has long relaxation times, and the defects are stable over several years.[11,36] Two millimeter cube of quartz glasses with known OH contents (160 ppm) were purchased (S-grade by TOSOH Quartz Co., Ltd) and irradiated using Cobalt-60 for 24 h to an estimated

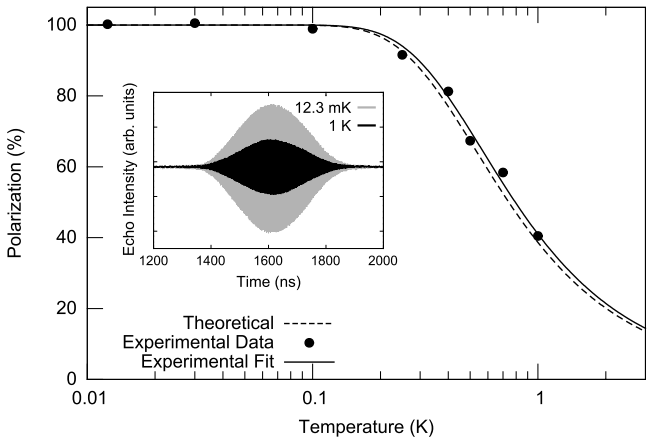

FIG. 4. Spin echo signal intensities were used to indicate thermal spin polarization of γ-irradiated quartz glass below 1 K. The inset image shows the echo signals down-converted to 300 MHz in time domain at 12.3 mK (gray line) and 1 K (black line). The experiment was conducted using single-shot measurements with TE_{011} cylindrical cavity at 0.6063 T. Signal intensities obtained at $T \leq 100$ mK were averaged together and assumed as $P = 100\%$. Experimental fit was plotted using $P(T) = P_0 \tanh\left(\frac{a}{T}\right)$, where a is the fitting parameter and $P_0 = 100\%$. Theoretical data were calculated using Eq. (1) with $B_0 = 0.6063$ T and is in good agreement with the experimental results.

dosage of 8 MGy to produce a spin density of about 10^{22} spins/m^3; the spin density was estimated by comparing it with DPPH using continuous wave EPR. For smaller sizes, the irradiated sample was broken into smaller pieces.

Next, the sample was fixed to a quartz glass rod using small amounts of cryogenic grease (Apiezon N grease by M & I Materials Ltd) and placed into the resonator (see Fig. 3). Grease was also applied between the glass rod and resonator's cover to help improve thermal conductivity for low temperature experiments. Care was taken to minimize the amount of grease inside the cavity due to lack of information regarding its loss tangent at 17 GHz at millikelvin temperatures (manufacturer rated loss tangent <0.0001, measured at 50 Hz at room temperature).

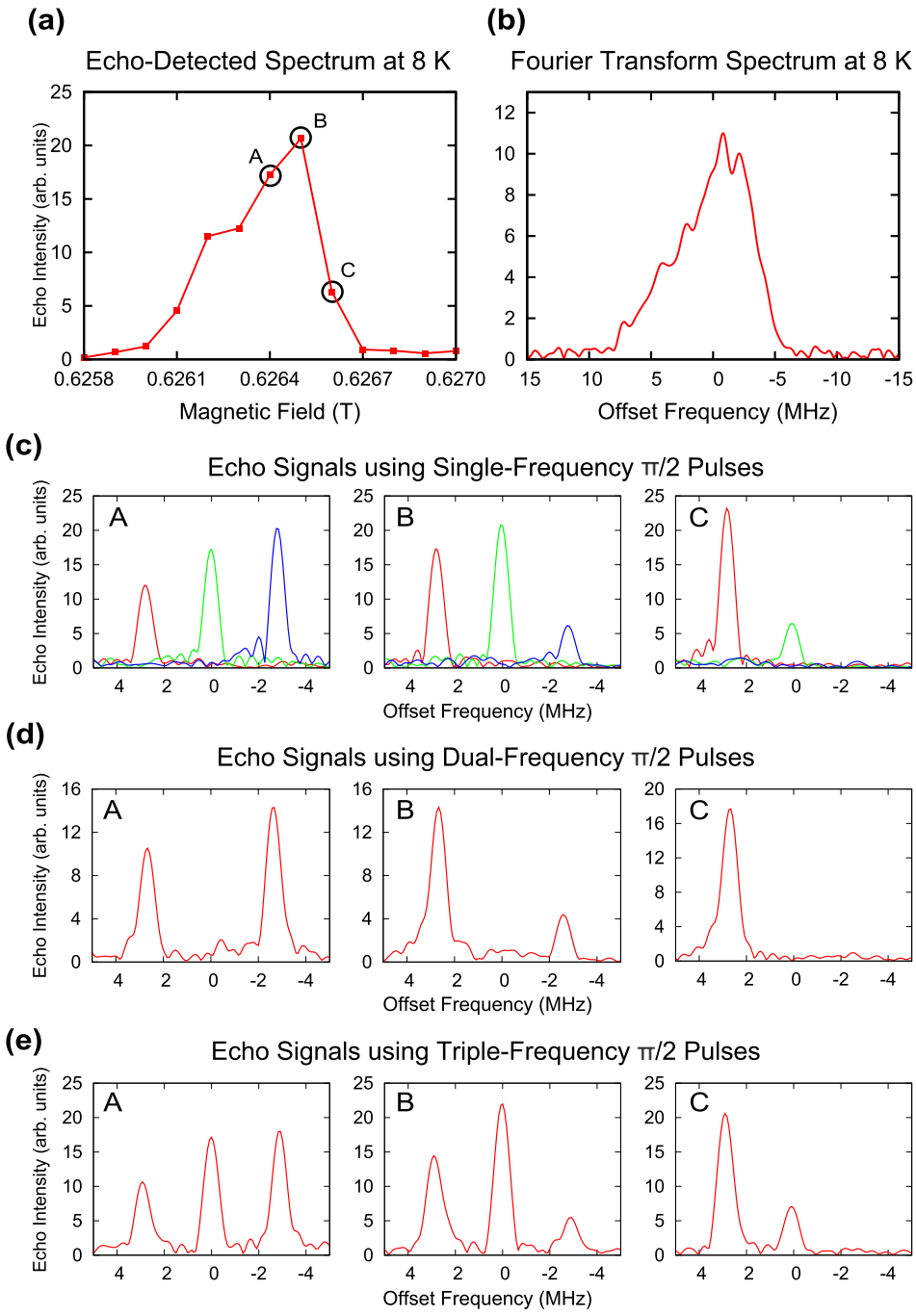

FIG. 5. Spin echo signals from γ-irradiated quartz at 8 K using the LGR. (a) Echo signal intensities obtained at various magnetic field strengths (the resolution of the magnet power supply was 1 G). Further experiments were carried out at 0.6264, 0.6265, and 0.6266 T, designated as "A," "B," and "C," respectively. (b) Echo spectrum obtained using a simple spin echo pulse at 0.6264 T (peak power entering the resonator = 600 mW, $\pi/2$ pulse duration = 22 ns). (c) Echo signals obtained using single-frequency $\pi/2$ Gaussian pulses; each color represents an independent echo signal obtained using different $\pi/2$ pulse frequencies. The red, green, and blue lines represent 2.8, 0, and −2.8 MHz offset frequencies, respectively. As an example, at magnetic field "A," the 2.8, 0, and −2.8 MHz offset frequencies correspond to echo signal intensities at 0.6263, 0.6264, and 0.6265 T, respectively. (d) Echo signals obtained using shaped pulses made by superposing two Gaussian $\pi/2$ pulses of different offset frequencies (2.8 and −2.8 MHz). (e) Echo signals obtained using shaped pulses made by superposing three Gaussian $\pi/2$ pulses of different offset frequencies (2.8, 0, and −2.8 MHz). The asymmetrical echo signal intensities observed in (c)–(e) were due to the distribution of spin packets in the sample.

Two types of resonators were built and tested down to millikelvin temperatures: a TE_{011} cylindrical cavity and a loop-gap resonator (LGR) consisting of 3 loops and 2 gaps (see Fig. 3). Both transmission-type resonators were made of oxygen-free copper (minimum purity of 99.96% based on JIS C1020P standards). In the dilution refrigerator, the resonators were connected to waveguides, which were then connected to the superconducting cables via cryogenic coaxial cables (see Fig. 2). For both resonators, irises were used to couple the waveguide to the resonators.

The resonant frequencies of the sample-loaded cylindrical cavity and LGR at room temperature were 16.89 GHz and 17.48 GHz, which increased slightly to 16.93 GHz and 17.5 GHz at around 10 mK, respectively. At room temperature, the sample-loaded TE_{011} cylindrical cavity was overcoupled (Q factor ≈ 800), whereas the sample-loaded LGR was almost critically coupled (Q factor ≈ 410). When cooled down to low temperatures, there was no noticeable improvement in the cylindrical cavity's Q factor; any improvement was hidden by the initial overcoupled condition of the resonator. However, the LGR's Q factor increased to around 715 at 12.5 mK.

IV. EXPERIMENTS AND RESULTS

A. Thermal polarization below 1 K

In order to observe thermal spin polarization with decreasing temperature, signal intensity was used as a direct indication of spin polarization. Single-shot measurements using simple spin echo pulses were carried out at different temperatures from 12.3 mK to 1 K. This experiment was carried out using TE_{011} cylindrical cavity at $B_0 = 0.6063$ T with π pulse duration = 200 ns (pulse peak power at the TWTA output was about 33 W and was attenuated to 815 mW at the cavity) and the duration of free evolution τ = 1650 ns. This corresponds to a microwave power-to-field conversion efficiency Λ, of around 1 G/$\sqrt{\text{W}}$.[35,37] The signal intensities were sufficiently strong that only one amplifier was used in the spectrometer's receiver (the second BZ1218LC1 LNA and AD8353 amplifiers were removed).

From the data, we observed increasing spin echo signal intensities with decreasing temperature, which matches well with the expected increase of thermal spin polarizations in Eq. (1). Here, $(\hbar\gamma_e B_0)/(2k_B) = 0.408$, while the fitting parameter $a = 0.436$. Through experimental data fit, the estimated polarization was $P \approx 99\%$ at T = 100 mK (see Fig. 4). For $T \leq 100$ mK, echo signal intensities did not increase significantly.

B. Triple-frequency excitations at millikelvin temperatures

To demonstrate the capability of the proposed setup, we generated a triple-frequency shaped pulse to excite several spin packets simultaneously at millikelvin temperatures. γ-irradiated quartz glass was suitable for this experiment since it is an inhomogeneously broadened sample. First, experiments were conducted using single-shot measurements at 8 K, which was the highest attainable temperature for the dilution refrigerator. These included Rabi frequency measurements, pulse power calibration, and acquiring the echo-detected spectrum of the sample (see Figs. 5(a) and 5(b)). Using saturation recovery, the spin-lattice relaxation time constant, T_1, was measured to be around 5.5, 7.9, and 13 s at 8, 7, and 6 K, respectively (these data can be fitted using the function $2800 \times T^{-3}$). With approximately 600 mW of pulse peak power entering into the resonator (6.3 W at the TWTA output), the Rabi frequency was 11.3 MHz ($\Lambda \approx 5.2$ G/$\sqrt{\text{W}}$). At 8 K, signal intensities were sufficiently strong that the AD8353 amplifier was removed from the receiver (refer to Fig. 1).

Next, single-frequency shaped $\pi/2$ pulses were used to obtain narrow-band echo signals at different offset frequencies (see Fig. 5(c)). Narrow-band excitations were achieved using long, low power $\pi/2$ pulses and to further improve frequency-selectivity, these pulses were shaped as Gaussian pulses.[5] The full width half maximum of the Gaussian envelope was 1397 ns. The incident peak power at the maximum amplitude of the Gaussian pulse was estimated to be 0.14 mW.[38] The π pulse, on the other hand, remained on-resonance (peak power entering the resonator = 600 mW, pulse duration = 44 ns). By comparing echo intensities at different B_0 (Fig. 5(c)), we found that the asymmetric intensities were due to the distribution of spin packets in the sample.

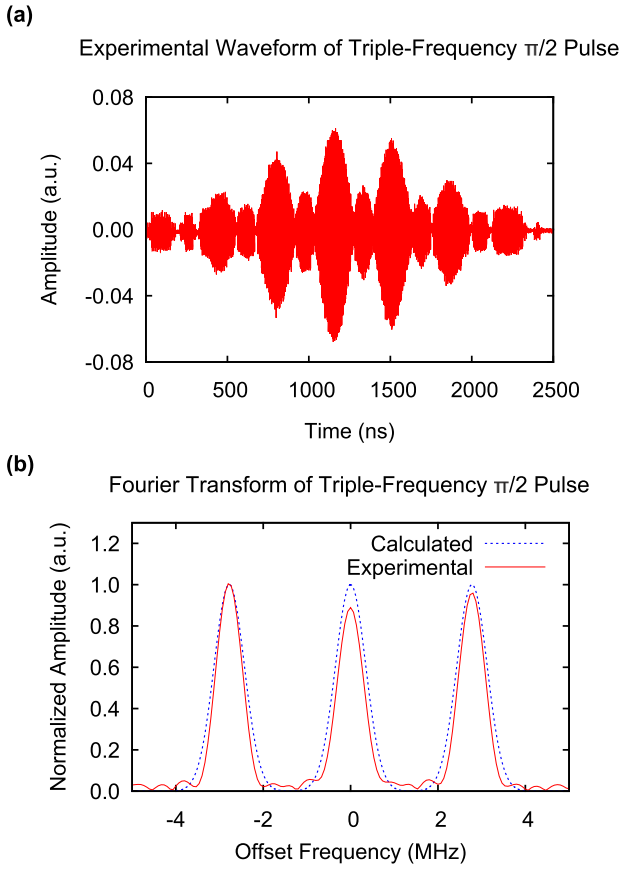

FIG. 6. The triple-frequency $\pi/2$ shaped pulse (2.8, 0, and −2.8 MHz) in (a) time and (b) frequency domain. The $\pi/2$ pulse waveform was numerically designed (represented as a broken blue line in (b)) and compiled using a home-built software compiler. The experimental waveform was obtained via direct feedback from the transmitter output to receiver input, without using the traveling-wave tube amplifier.

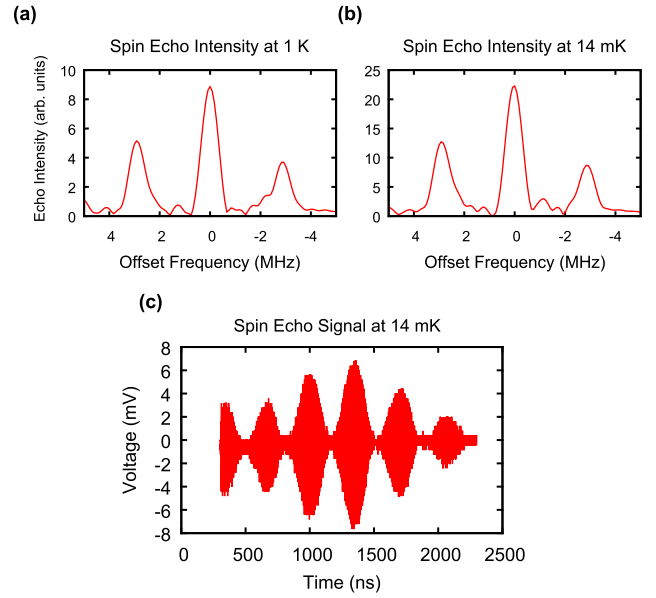

FIG. 7. Spin echo signal intensities obtained at $B_0 = 0.6265$ T using a triple-frequency $\pi/2$ pulse (2.8, 0, and −2.8 MHz) on γ-irradiated quartz in a loop gap resonator at (a) 1 K and (b) 14 mK. The spin echo signal obtained at 14 mK in time domain is presented in (c). Signal acquisition started at 350 ns from the end of the last pulse, for a duration of 2000 ns. The interference pattern of the echo signal is evidence of *coherent manipulation* of each spin packet.

By superposing two or three of the different single-frequency Gaussian $\pi/2$ pulses, dual- and triple-frequency shaped pulses were created (see Fig. 6). These superposed shaped pulses were used to obtain dual- and triple-frequency excitations at 8 K (see Figs. 5(d) and 5(e), respectively), which were phase coherent (see discussion in Sec. V). For these experiments, the π pulse was not changed so as to have a broad bandwidth, which in turn was limited by the resonator's bandwidth. Finally, the experiments were repeated at 1 K and 14 mK using single-shot measurements with only one amplifier in the receiver (the second BZ1218LC1 LNA and AD8353 amplifier were removed). Similarly, three well-resolved excitations were obtained at 1 K and 14 mK (Fig. 7).

V. DISCUSSION AND SUMMARY

Pulsed EPR below 1 K remains largely unexplored but experiments at millikelvin temperatures may be beneficial to study the dynamics and properties of materials near the ground state in the fields of quantum chemistry, organic magnetism and electronics, protein research, and so on.[30,31,39–42] Furthermore, for our target application of quantum computation and quantum information processing, lowering temperature reduces entropy and initializes the qubits. To that end, we have developed an arbitrary waveform pulsed EPR spectrometer at Ku band for millikelvin experiments. The ability to generate arbitrary waveform pulses is equally crucial for our target application, where precise spin control may take the form of composite pulses, multi-frequency shaped pulses or pulses designed using numerical calculations, or optimal control theory.[1,2,8,43–45] Additionally, the proposed setup would also be useful for other EPR experiments. AWG-based spectrometers have been shown to improve the modulation depth of pulsed electron-electron double resonance (PELDOR) experiments.[18] Furthermore, it has been suggested that through precise excitation, double quantum coherence (DQC) experiments could outperform PELDOR's measurements.[17,46] The ability to create selective and multi-frequency pulses may also be useful to investigate multi-spin samples and to selectively address different qubits in a quantum computation experiment.[47–50]

Here, we have demonstrated (1) almost unity polarization using simple spin echo pulses and (2) the ability to create arbitrary waveform pulses, i.e., shaped and multi-frequency pulses, for experiments at millikelvin temperatures. Evidence of almost unity polarization was based on the increment of echo signal intensities from 1 K to 12.3 mK, which is in good agreement with theoretical predictions. The highest demonstrated polarization here was at least 99% although the calculated polarization at 100 mK was 99.94%, which increased to 99.9999% at 50 mK. Experimentally, signal intensities below 100 mK ($P > 99\%$) were indistinguishable due to the receiver's limited dynamic range and instrumental stability between measurements. Therefore, accurate measurement of spin polarization above 99% for $T \leq 100$ mK remains an open issue for future studies. As far as we know, the lowest temperature reported for pulsed EPR with ensembles was carried out at 200 mK using phosphorus donor atoms (^{31}P) in silicon (Si:P) at a frequency of 9.4 GHz.[51] At an estimated magnetic field of 0.36 T ($g = 1.9989$ for Si:P),[52] the polarization was estimated to be around 81% at the reported temperature.

Using the proposed setup, we have carried out spin echo experiments down to 14 mK, using a triple-frequency shaped $\pi/2$ pulse and successfully obtained three well-resolved excitations over an 8 MHz bandwidth. It is also worth noting that all three excitations were phase coherent to each other (see Fig. 7(c)). While phase coherence between two frequencies is not a minor task for conventional spectrometers, it is essential for some EPR experiments, e.g., for soft pulse electron-spin-echo-envelope modulation (soft ESEEM) spectroscopy.[53] The proposed setup described here is readily extendable to more frequencies without significant modification to the setup. Using a multi-frequency shaped pulse, somewhat similar to a frequency comb, it may be possible to obtain many well-resolved excitations, spread out evenly across the entire spectrum of an inhomogeneously broadened sample (instead of only three well-resolved excitations demonstrated here). The proposed spectrometer has sufficient bandwidth for such tasks and much more; the main hindrance here was the resonator's limited bandwidth. A common solution is to decrease the resonator's Q factor either by overcoupling the resonator or by inserting lossy materials. These techniques, however, will undoubtedly trade off excitation strength for a larger bandwidth at the same incident power. Alternatively, our previously proposed room temperature stripline resonator provides for a larger bandwidth (up to 500 MHz) and a stronger excitation strength (up to 75 G/$\sqrt{\text{W}}$ or 210 MHz/$\sqrt{\text{W}}$).[35] Research into a new stripline resonator for experiments in the dilution refrigerator is already in progress.

Even with a broadband resonator, short pulses will still deform due to linear or nonlinear distortion.[54] Linear distortion

tends to occur inside a resonator due to amplitude and phase transients of the applied pulse, which can be corrected using an AWG-based spectrometer.[16,55] On the other hand, nonlinear effects are commonly caused by mixers and TWTAs, which are time and temperature dependent. Nonlinear effects were observed in the triple-frequency excitation experiments but not described here. A promising solution, made possible by the AWG in the spectrometer, is to employ linearization techniques frequently used for radio-frequency power amplifiers such as digital predistortion or feedback techniques.[56,57] Further investigation to employ these techniques to precisely control spins is reserved for future work.

ACKNOWLEDGMENTS

The authors would like to thank Associate Professor Dr. Chihiro Yamanaka of Osaka University for his technical assistance and Sanken, The Institute of Scientific and Industrial Research (I.S.I.R) of Osaka University for their assistance and for using their Cobalt-60 irradiation facilities. We are grateful to Professor Dr. Kev M. Salikhov for his valuable suggestion and fruitful discussion. This work was supported by CREST program, Japan Science and Technology Agency (JST), the Ministry of Education, Culture, Sports, Science and Technology (MEXT) Grant-in-Aid for Scientific Research on Innovative Areas No. 21102004 and the Funding Program for World-Leading Innovating R&D on Science and Technology (FIRST program). Y.S.Y is also financially supported by The Malaysia Ministry of Education (MoE).

[1]L. M. K. Vandersypen and I. L. Chuang, Rev. Mod. Phys. **76**, 1037 (2005).
[2]H. K. Cummins, G. Llewellyn, and J. A. Jones, Phys. Rev. A **67**, 042308 (2003).
[3]S. Wimperis, J. Magn. Reson., Ser. A **109**, 221 (1994).
[4]R. Tycko, Phys. Rev. Lett. **51**, 775 (1983).
[5]C. Bauer, R. Freeman, T. Frenkiel, J. Keeler, and A. Shaka, J. Magn. Reson. (1969) **58**, 442 (1984).
[6]W. S. Warren, J. Chem. Phys. **81**, 5437 (1984).
[7]S. L. Patt, J. Magn. Reson. (1969) **96**, 94 (1992).
[8]N. Khaneja, T. Reiss, C. Kehlet, T. Schulte-Herbrüggen, and S. J. Glaser, J. Magn. Reson. **172**, 296 (2005).
[9]V. M. R. Kakita, E. Kupče, and J. Bharatam, J. Magn. Reson. **251**, 8 (2015).
[10]L. M. Vandersypen, M. Steffen, G. Breyta, C. S. Yannoni, M. H. Sherwood, and I. L. Chuang, Nature **414**, 883 (2001).
[11]G. A. Rinard, R. W. Quine, J. R. Harbridge, R. Song, G. R. Eaton, and S. S. Eaton, J. Magn. Reson. **140**, 218 (1999).
[12]N. Devasahayam, R. Murugesan, K. Matsumoto, J. Mitchell, J. Cook, S. Subramanian, and M. Krishna, J. Magn. Reson. **168**, 110 (2004).
[13]I. Gromov, B. Glass, J. Keller, J. Shane, J. Forrer, R. Tschaggelar, and A. Schweiger, Concepts Magn. Reson., Part B: Magn. Reson. Eng. **21**, 1 (2004).
[14]J. S. Hodges, J. C. Yang, C. Ramanathan, and D. G. Cory, Phys. Rev. A **78**, 010303 (2008).
[15]M. Tseitlin, R. W. Quine, G. A. Rinard, S. S. Eaton, and G. R. Eaton, J. Magn. Reson. **213**, 119 (2011).
[16]P. E. Spindler, Y. Zhang, B. Endeward, N. Gershernzon, T. E. Skinner, S. J. Glaser, and T. F. Prisner, J. Magn. Reson. **218**, 49 (2012).
[17]T. Kaufmann, T. J. Keller, J. M. Franck, R. P. Barnes, S. J. Glaser, J. M. Martinis, and S. Han, J. Magn. Reson. **235**, 95 (2013).
[18]A. Doll, S. Pribitzer, R. Tschaggelar, and G. Jeschke, J. Magn. Reson. **230**, 27 (2013).
[19]Bruker Corporation, Commercial Spinjet-AWG EPR Accessory System, 2014.
[20]A. Doll and G. Jeschke, J. Magn. Reson. **246**, 18 (2014).
[21]D. G. Cory, R. Laflamme, E. Knill, L. Viola, T. Havel, N. Boulant, G. Boutis, E. Fortunato, S. Lloyd, R. Martinez *et al.*, Fortschr. Phys. **48**, 875 (2000).
[22]S. C. Benjamin, A. Ardavan, G. A. D. Briggs, D. A. Britz, D. Gunlycke, J. Jefferson, M. A. Jones, D. F. Leigh, B. W. Lovett, A. N. Khlobystov *et al.*, J. Phys.: Condens. Matter **18**, S867 (2006).
[23]J. A. Jones, Prog. Nucl. Magn. Reson. Spectrosc. **38**, 325 (2001).
[24]P. O. Boykin, T. Mor, V. Roychowdhury, F. Vatan, and R. Vrijen, Proc. Natl. Acad. Sci. U. S. A. **99**, 3388 (2002).
[25]M. G. Dutt, L. Childress, L. Jiang, E. Togan, J. Maze, F. Jelezko, A. Zibrov, P. Hemmer, and M. Lukin, Science **316**, 1312 (2007).
[26]A. G. Fowler, D. S. Wang, C. D. Hill, T. D. Ladd, R. Van Meter, and L. C. Hollenberg, Phys. Rev. Lett. **104**, 180503 (2010).
[27]D. S. Wang, A. G. Fowler, and L. C. Hollenberg, Phys. Rev. A **83**, 020302 (2011).
[28]K. Fujii, M. Negoro, N. Imoto, and M. Kitagawa, Phys. Rev. X **4**, 041039 (2014).
[29]G. W. Morley, L.-C. Brunel, and J. van Tol, Rev. Sci. Instrum. **79**, 064703 (2008).
[30]S. Takahashi, R. Hanson, J. van Tol, M. S. Sherwin, and D. D. Awschalom, Phys. Rev. Lett. **101**, 047601 (2008).
[31]E. Reijerse, P. P. Schmidt, G. Klihm, and W. Lubitz, Appl. Magn. Reson. **31**, 611 (2007).
[32]F. H. Cho, V. Stepanov, and S. Takahashi, Rev. Sci. Instrum. **85**, 075110 (2014).
[33]Maximum output power was 1.5 kW, which was reserved mostly for room temperature experiments.
[34]O. V. Lounasmaa, O. Louasmaa, and O. Lounasmaa, in *Experimental Principles and Methods Below 1 K* (Academic Press, London, 1974), Vol. 8.
[35]Y. S. Yap, H. Yamamoto, Y. Tabuchi, M. Negoro, A. Kagawa, and M. Kitagawa, J. Magn. Reson. **232**, 62 (2013).
[36]G. R. Eaton, S. S. Eaton, R. W. Quine, D. Mitchell, V. Kathirvelu, and R. T. Weber, J. Magn. Reson. **205**, 109 (2010).
[37]J. S. Hyde, W. Froncisz, and T. Oles, J. Magn. Reson. (1969) **82**, 223 (1989).
[38]The estimation was done by measuring the Rabi oscillation using rectangular pulses with the same peak power and calculating based on the resonator efficiency.
[39]T. Fujito, Bull. Chem. Soc. Jpn. **54**, 3110 (1981).
[40]M. Oshikawa and I. Affleck, Phys. Rev. Lett. **82**, 5136 (1999).
[41]T. Tokumoto, J. Brooks, Y. Oshima, E. Choi, L. Brunel, H. Akutsu, T. Kaihatsu, J. Yamada, and J. van Tol, Phys. Rev. Lett. **100**, 147602 (2008).
[42]M. V. Fedin, S. L. Veber, G. V. Romanenko, V. I. Ovcharenko, R. Z. Sagdeev, G. Klihm, E. Reijerse, W. Lubitz, and E. G. Bagryanskaya, Phys. Chem. Chem. Phys. **11**, 6654 (2009).
[43]N. C. Jones, R. Van Meter, A. G. Fowler, P. L. McMahon, J. Kim, T. D. Ladd, and Y. Yamamoto, Phys. Rev. X **2**, 031007 (2012).
[44]J. A. Jones, J. Indian Inst. Sci. **89**, 303 (2009).
[45]P. Cerfontaine, T. Botzem, D. P. DiVincenzo, and H. Bluhm, Phys. Rev. Lett. **113**, 150501 (2014).
[46]Y.-W. Chiang, P. P. Borbat, and J. H. Freed, J. Magn. Reson. **172**, 279 (2005).
[47]S. Lloyd *et al.*, Science **261**, 1569 (1993).
[48]G. Jeschke, M. Sajid, M. Schulte, and A. Godt, Phys. Chem. Chem. Phys. **11**, 6580 (2009).
[49]Y. Morita, Y. Yakiyama, S. Nakazawa, T. Murata, T. Ise, D. Hashizume, D. Shiomi, K. Sato, M. Kitagawa, K. Nakasuji *et al.*, J. Am. Chem. Soc. **132**, 6944 (2010).
[50]A. Olankitwanit, V. Kathirvelu, S. Rajca, G. R. Eaton, S. S. Eaton, and A. Rajca, Chem. Commun. **47**, 6443 (2011).
[51]W. D. Hutchison, L. K. Alexander, N. Suwuntanasarn, and G. N. Milford, in *Proceedings of the 34th Annual Condensed Matter and Materials Meeting* (Australian Institute of Physics, 2010), article 9; preprint arXiv:1002.4069 (2010).
[52]N. Suwuntanasarn, "Magnetic resonance studies of issues critical to solid state quantum computer," Ph.D. thesis, University of New South Wales–Australian Defence Force Academy, School of Physical, Environmental, and Mathematical Sciences, 2008.
[53]A. Schweiger, C. Gemperle, and R. Ernst, J. Magn. Reson. (1969) **86**, 70 (1990).
[54]In some cases, this problem can be rectified by using long, low-powered modulated pulses, which are intrinsically robust against distortion.[18,20]
[55]Y. Tabuchi, M. Negoro, K. Takeda, and M. Kitagawa, J. Magn. Reson. **204**, 327 (2010).
[56]K. Mekechuk, W.-J. Kim, S. P. Stapleton, and J. H. Kim, High Freq. Electron. **3**(4), 18 (2004).
[57]J. L. Dawson and T. H. Lee, in *Proceedings of the American Control Conference* (IEEE, 2004), Vol. 1, pp. 361–366.